Electronic Structure and Optical Gain of InNBiAs/InP Pyramidal Quantum Dots

Zhigang Song[a,b], Sumanta Bose[b], W. J. Fan[b,c], X. H. Tang[b], D. H. Zhang[b], S. S. Li[a]

[a] *SKLSM, Institute of Semiconductors, Chinese Academy of Sciences, China*
[b] *School of Electrical and Electronic Engineering, Nanyang Technological University, Singapore*
[c] *Corresponding author: ewjfan@ntu.edu.sg*

Abstract

Dilute bismide alloys and dilute nitride alloys have garnered increasing research interest over the past few years, as it promises increased engineering flexibility in the design of advanced compound semiconductor heterostructure devices. Key device parameters such as lattice constant, bandgap and band offsets can be controlled with greater precision, and this leads to better performance for a wide range of electronic and optoelectronic devices. For dilute nitride alloys, band anticrossing effects are produced due to the coupling of their resonant states with the conduction band states. This lowers the conduction band edge energy. Likewise, the coupling of the resonant states of dilute bismide with the valence band states results in the valence band anticrossing and the valence band edge energy rises. Additionally, the effective bandgap may fall below the spin-orbital-splitting energy, thus inhibiting Auger recombination. This makes them excellent candidates for optoelectronic device applications. In this work, the electronic bandstructure and optical gain of InNBiAs/InP pyramidal quantum dots are investigated using the 16-band $\boldsymbol{k}\cdot\boldsymbol{p}$ model with constant strain. The effective bandgap falls as we increase the composition of nitrogen and bismuth. With an appropriate choice of composition of doped atoms, we can tune the emission wavelength in the range of 2–5μm suitable for mid-infrared device applications. Additionally, we observe the size effect by tuning the size of quantum dot.

Keywords: Dilute nitrogen, Dilute bismuth, Quantum dot, Band anticrossing, Optical gain, Size effect

1. Introduction

Owing to the increased engineering flexibility in the design of advanced compound semiconductor heterostructure devices, dilute bismide alloys and dilute nitride alloys have garnered increasing research interest over the past few years [1, 2, 3, 4]. Increased control over key device parameters such as lattice constant, bandgap and band offsets opens the door to improved performance for a wide range of electronic and optoelectronic devices. For dilute nitride alloys, the *s*-like resonant states couples with the conduction band (CB) states and produce the band anticrossing (BAC) effects [5, 6]. This causes the CB band edge to get lowered compared to the unalloyed case. Similarly, for dilute bismide alloys, the valence band (VB) edge is lifted due to the valence band anticrossing (VBAC) resulting from coupling between the *p*-like resonant states and VB states [7]. In addition, the spin-orbital-splitting energy Δ_{SO} can exceed the bandgap in dilute bismuth alloy which can inhibit the Auger recombination [8, 9], making it an excellent candidate for optoelectronic device applications.

Here, we investigate the electronic bandstructure and optical gain of InNBiAs/InP quantum dot (QD) by the 16-band $\boldsymbol{k}\cdot\boldsymbol{p}$ model. In comparison to the bulk and quantum well system, the QD is confined in three dimension and the energy level is discrete.

2. Theoretical model

The 10-band $\boldsymbol{k}\cdot\boldsymbol{p}$ model used to study the nitrogen-doped QDs are based on the 8-band model extended by introducing the local nitrogen resonant state (two additional bands). Similarly, to investigate the bismuth-doped and nitrogen-doped QDs simultaneously, additional bands have to be added in the model to describe and study the effects of bismuth. Unlike the *s*-like states introduced by dilute nitride, the dilute bismide results in *p*-like states, which means that six states should be considered with the spin freedom including the *SO* coupling which is ignored in

the O'Reilly 14-band model for dilute bismide-nitride semiconductors. In view of the above consideration, we have constructed a 16-band model to study the $InN_xBi_yAs_{1-x-y}$/InP system. The 16-band Hamiltonian is represented in the Bloch function basis $|S,\uparrow\rangle, |S,\downarrow\rangle, |11,\uparrow\rangle, |10,\uparrow\rangle, |1-1,\uparrow\rangle, |11,\downarrow\rangle, |10,\downarrow\rangle, |1-1,\downarrow\rangle, |S_N,\uparrow\rangle, |S_N,\downarrow\rangle, |11_{Bi},\uparrow\rangle, |10_{Bi},\uparrow\rangle, |1-1_{Bi},\uparrow\rangle, |11_{Bi},\downarrow\rangle, |10_{Bi},\downarrow\rangle, |1-1_{Bi},\downarrow\rangle$ as

$$H_{16} = \begin{pmatrix} H_{10\times10} & H_{10\times6} \\ H_{6\times10} & H_{6\times6} \end{pmatrix} + V_{QD}, \tag{1}$$

where $H_{10\times10}$ is the 10-band model to describe the nitrogen-doped system, $H_{6\times6}$ is the 6-band model to describe the resonant bismuth states, $H_{10\times6}$ is the coupling between the valence band and bismuth states, and the V_{QD} is the confinement potential of the system, which is zero within the QD. As we use the $|10\rangle, |1-1\rangle, |11\rangle$ basis for the p-like states instead of $|HH\rangle, |LH\rangle, |SO\rangle$, the form of Hamiltonian is different form the O'Reilly's model and can be transformed into it under an unitary transformation. The details of the every element in $H_{10\times10}$, $H_{6\times6}$, $H_{10\times6}$, etc is as described in our previous work [10].

The optical gain spectrum with homogeneous broadening is calculated as [10]

$$G(E) = \frac{\pi e^2\hbar}{m_0^2\varepsilon_0 n_r cE}\sum_{n_c,n_v}\frac{1}{V}|M^{cv}|^2(f_c+f_v-1)\frac{1}{\pi}B_{cv}(E-E_{cv}) \tag{2}$$

where E_{cv} is the transition energy and f_c and f_v are the Fermi-Dirac distribution for electrons and holes in CB and VB respectively. The M^{cv} is the optical transition matrix element and can be calculated as [11]

$$M_i^{cv} = \left\langle \psi_{n_v,k}\left|\widehat{p_i}\right|\psi_{n_c,k}\right\rangle, i = x,y,z \tag{3}$$

where $\widehat{p_i}$ is the momentum operator, and $\psi_{n_v,k}(\psi_{n_c,k})$ is the hole (electron) wave function. The calculation of the M^{cv} is shown in details in our previous work [10, 12].

3. Results and Discussion

The geometry schematic of $InN_xBi_yAs_{1-x-y}$/InP QD is shown in Fig. 1 with the direction of pyramid growth along the positive z axis. The doped nitrogen and bismuth atoms are distributed uniformly in crystal throughout the QD. The detail of the structure can be found in our previous work [10]. Here the H represents the height of the QD which takes the lattice constant (a) as the unit length. In this work we will study the InNBiAs QDs of different heights (H). The interaction between the doped atoms is not taken into consideration.

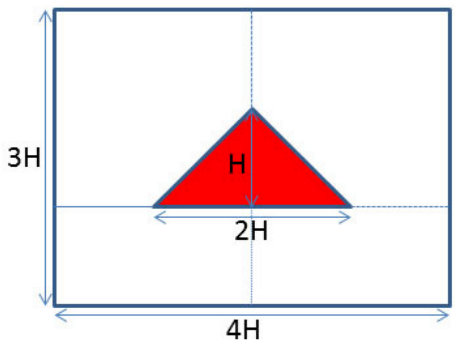

Figure 1: The geometry schematic of the pyramidal QDs in the side view. The height (H), width (2H) and dimensions of the system are an integer multiple of the lattice constant (a).

First we investigate the energy level and related distribution of compositions for a typical QD. From Fig. 2 we can see that the majority of CB1 is electron state and the majority of VB1 is heavy hole state. Bismuth resonant states and nitrogen resonant states also have been mixed.

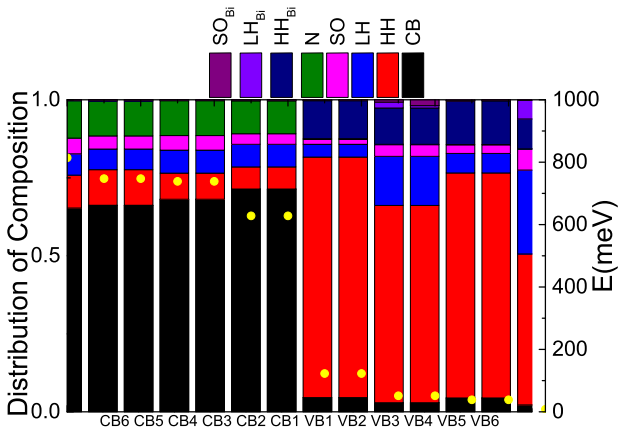

Figure 2: Electronic bandstructure and probability in band-mixing between electron, heavy-hole, light-hole, split-off-hole and N and Bi holes. The yellow dots in the bar represents the energy level of QD. The concentration of nitrogen and bismuth are 2.86% each and the height of QD is H=12a.

Another important factor for QD is the QD size i.e the height. Fig. 3 shows the size effect for QD. The band edge of the CB goes down, while for the VB goes up with increasing Bi concentration for three different heights of QD (H = 12a, 16a and 20a, as shown) when the nitrogen concentration is fixed at 1.6%. If we fix the bismuth concentration instead, we would observe that the bandgap would decrease as the height of QD is increases.

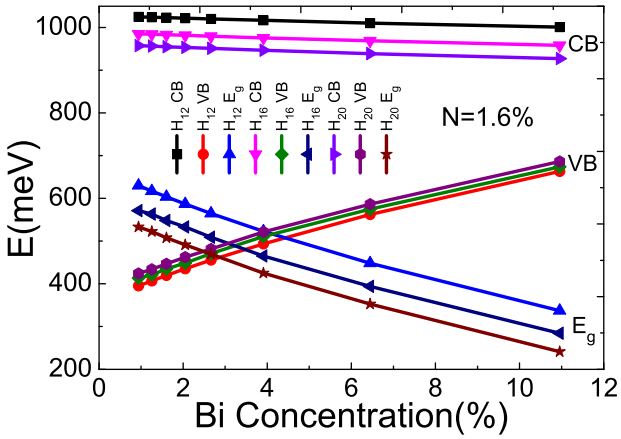

Figure 3: The variation in CB1, VB1 and bandgap E_g for InNBiAs/InP QDs of H = 12a, 16a and 20a for varying composition of doped Bi and fixed N composition = 1.6%. We see that the range of the bandgap (emission energy) varies from ~250 to ~650 meV, making the InNBiAs/InP QDs suitable for mid-infrared (2–5 μm) applications.

In addition, we study the variation of the bandgap and strain with varying nitrogen and bismuth concentration. The results can be seen in Fig. 4. The initial idea to utilize the BAC and VBAC to realize mid-infrared emission (2–5 μm), and Fig. 3 shows it can be achieved. A suitable composition from the bandgap range of 250 to 650 meV could be chosen from Fig. 4. Meanwhile, doping nitrogen can introduce tensile strain, while bismuth can introduce compressive strain. Therefore, the strain in QD can be tuned by choosing appropriate concentration of doped atoms in order to meet the requirements of lattice matching for material growth [13].

Finally, the most important factor for lasers is the optical gain. Fixing the nitrogen concentration, we show the optical gain spectrum for varying bismuth concentration in Fig. 5. Additionally, we tune the carrier densities and investigate the variation of gain as shown. The magnitude of transverse magnetic (TM) mode gain is relatively smaller compared to the magnitude of transverse electric (TE) mode gain. The position of the first peak experiences a red-shift as the Bi concentration increases.

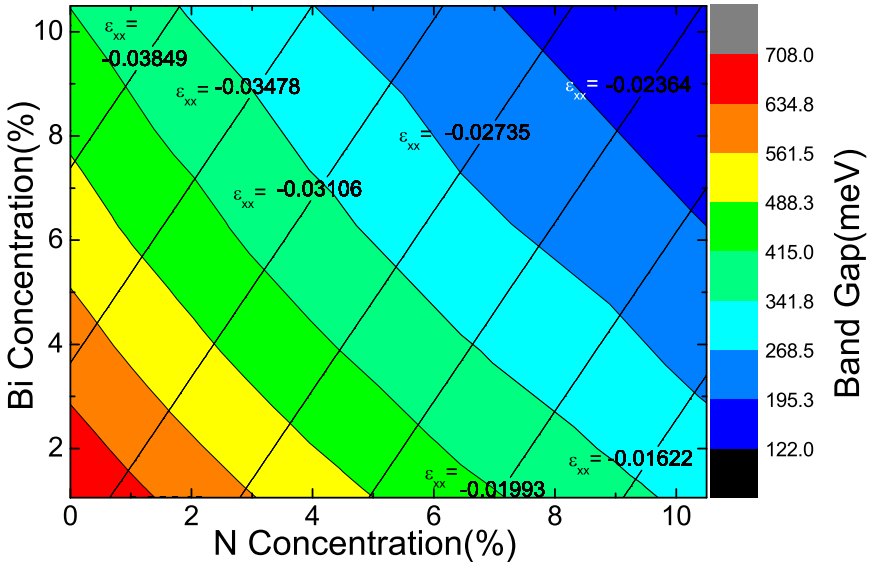

Figure 4: Variations in the bandgap (E_g) of $InN_xBi_yAs_{1-x-y}$ pseudomorphically grown on InP at 300 K vs. N and Bi composition (%). The strain component ε_{xx} is mentioned.

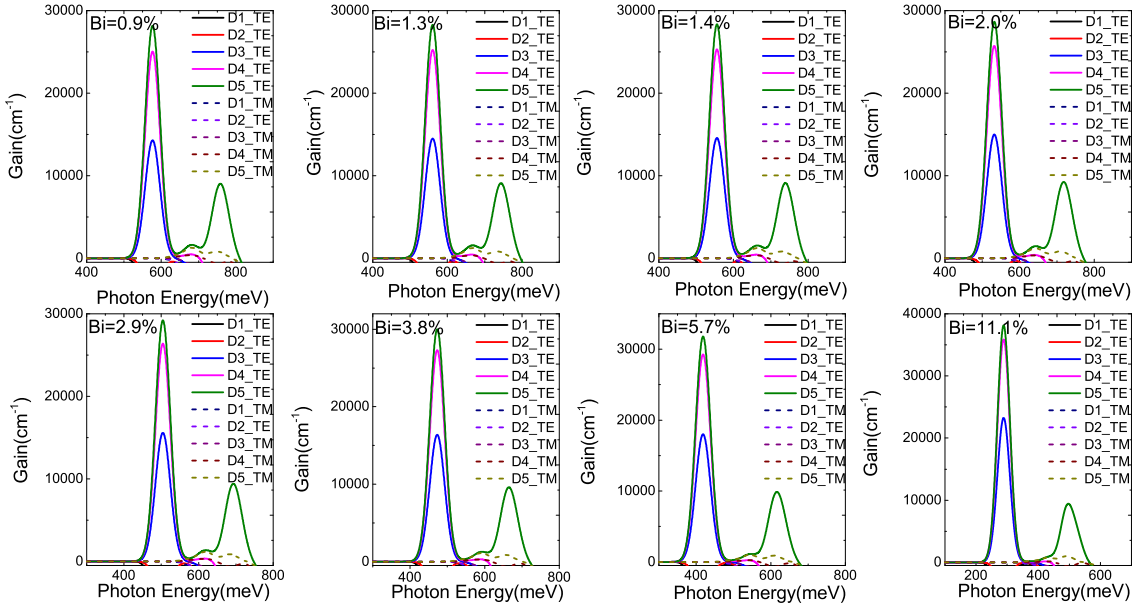

Figure 5: TE and TM mode optical gain for InNBiAs/InP QDs for varying injection carrier density from 1 to 5 $\times 10^{18}$ cm^{-3}. The Bi composition is varied from 0.9% to 11.1%, while the N composition is fixed at 2.9%. The height of QD is H=12a.

4. Summary and Conclusion

We have investigated the electronic bandstructure and optical gain of InNBiAs/InP QD. Utilizing the BAC and VBAC effects, we can achieve the goal that the emission wavelength of laser can exceed 2μm while meeting the strain requirements for suitable material growth. We observe that, with an appropriate choice of N and Bi doping composition, we can tune the emission wavelength in the range of 2–5 μm suitable for mid-infrared device applications, such as guided missile technology, spectroscopy of trace gases and more recent medical applications such as less-invasive, high-precision, laser surgery. One of the important characteristics of the III-V semiconductor based mid-infrared laser structures is that it possesses strong differences in band gap energy and band discontinuity allowing the formation of deep confining QW in the laser's active region, which cannot be obtained by using group IV based semiconductors. With the advancement of epitaxy growth techniques, it is possible to fabricate high quality III-V based quantum well structures for mid-IR lasers.

5. References

[1] H. Okamoto, K. Oe, Structural and Energy-Gap Characterization of Metalorganic-Vapor-Phase-Epitaxy-Grown InAsBi, Japanese Journal of Applied Physics 38 (2S) (1999) 1022.
URL http://stacks.iop.org/1347-4065/38/i=2S/a=1022

[2] P. T. Webster, N. A. Riordan, S. Liu, E. H. Steenbergen, R. A. Synowicki, Y.-H. Zhang, S. R. Johnson, Measurement of InAsSb bandgap energy and InAs/InAsSb band edge positions using spectroscopic ellipsometry and photoluminescence spectroscopy, Journal of Applied Physics 118 (24) (2015) 245706. doi:10.1063/1.4939293.

[3] P. T. Webster, A. J. Shalindar, N. A. Riordan, C. Gogineni, H. Liang, A. R. Sharma, S. R. Johnson, Optical properties of InAsBi and optimal designs of lattice-matched and strain-balanced III-V semiconductor superlattices, Journal of Applied Physics 119 (22) (2016) 225701. doi:10.1063/1.4953027.

[4] Z. Song, S. Bose, W. Fan, D. H. Zhang, Y. Y. Zhang, S. S. Li, Quantum spin Hall effect and topological phase transition in $InN_xBi_ySb_{1-x-y}$/InSb quantum wells, New Journal of Physics 19 (7) 073031. doi:10.1088/1367-2630/aa795c.

[5] J. Wu, W. Shan, W. Walukiewicz, Band anticrossing in highly mismatched III-V semiconductor alloys, Semiconductor Science and Technology 17 (8) (2002) 860.
URL http://stacks.iop.org/0268-1242/17/i=8/a=315

[6] J. Wu, W. Walukiewicz, E. E. Haller, Band structure of highly mismatched semiconductor alloys: Coherent potential approximation, Phys. Rev. B 65 (2002) 233210. doi:10.1103/PhysRevB.65.233210.

[7] K. Alberi, J. Wu, W. Walukiewicz, K. M. Yu, O. D. Dubon, S. P. Watkins, C. X. Wang, X. Liu, Y.-J. Cho, J. Furdyna, Valence-band anticrossing in mismatched iii-v semiconductor alloys, Phys. Rev. B 75 (2007) 045203. doi:10.1103/PhysRevB.75.045203.

[8] C. A. Broderick, M. Usman, E. P. O'Reilly, Derivation of 12- and 14-band k·p hamiltonians for dilute bismide and bismide-nitride semiconductors, Semiconductor Science and Technology 28 (12) (2013) 125025.
URL http://stacks.iop.org/0268-1242/28/i=12/a=125025

[9] C. A. Broderick, P. E. Harnedy, P. Ludewig, Z. L. Bushell, K. Volz, R. J. Manning, E. P. OReilly, Determination of type-I band offsets in $GaBi_xAs_{1-x}$ quantum wells using polarisation-resolved photovoltage spectroscopy and 12-band k·p calculations, Semiconductor Science and Technology 30 (9) (2015) 094009.
URL http://stacks.iop.org/0268-1242/30/i=9/a=094009

[10] Z.-G. Song, S. Bose, W.-J. Fan, S.-S. Li, Electronic band structure and optical gain of $GaN_xBi_yAs_{1-x-y}$/GaAs pyramidal quantum dots, Journal of Applied Physics 119 (14) (2016) 143103. doi:10.1063/1.4945700.
URL http://dx.doi.org/10.1063/1.4945700

[11] S. Bose, S. Shendre, Z. Song, V. K. Sharma, D. H. Zhang, C. Dang, W. Fan, H. V. Demir, Temperature-dependent optoelectronic properties of quasi-2D colloidal cadmium selenide nanoplatelets, Nanoscale 9 (2017) 6595–6605. doi:10.1039/C7NR00163K.
URL http://dx.doi.org/10.1039/C7NR00163K

[12] S. Bose, Z. Song, W. J. Fan, D. H. Zhang, Effect of Lateral Size and Thickness on the Electronic Structure and Optical Properties of Quasi Two-dimensional CdSe and CdS Nanoplatelets, Journal of Applied Physics 119 (14) (2016) 143107. doi:10.1063/1.4945993.
URL http://dx.doi.org/10.1063/1.4945993

[13] W. J. Fan, S. Bose, D. H. Zhang, Electronic bandstructure and optical gain of lattice matched III-V dilute nitride bismide quantum wells for 1.55μm optical communication systems, Journal of Applied Physics 120 (9) (2016) 093111. doi:10.1063/1.4962214.
URL http://dx.doi.org/10.1063/1.4962214